THE ELECTROCHEMISTRY OF POROUS ZINC
II. THE POLARISATION BEHAVIOUR OF PLAIN AND POLYMER-BONDED MICROELECTRODES IN KOH SOLUTIONS

N A HAMPSON and A J S McNEIL

Department of Chemistry, Loughborough University of Technology, Loughborough, Leicestershire, LE11 3TU (U K)

(Received October 19, 1984, in revised form April 18, 1985)

Summary

The steady state and transient polarisation behaviour in 7M KOH solution of porous zinc incorporating a number of polymeric binders (including poly(styrene), poly(methyl methacrylate), poly(vinyl chloride), poly(carbonate), poly(vinyl acetate), poly(isoprene), poly(ethylene) and acrylonitrile styrene) has been studied. The rotating disc electrode technique can be applied, with care, to microscopically rough porous electrodes, and useful data can be obtained. The addition of polymer binder, via a soluble route, could suppress the rotation speed dependence of the anodic dissolution reaction, but at the expense of the electrode's current delivery. The polymer additions thus formed two classes. (1) those that had little effect on current output, and (2) those that reduced it significantly. This was also found to apply to the effects of the polymers on electrode cycling behaviour. Whilst large additions of polymer reduced the weight of zinc in the electrode, both steady state and transient polarisation measurements demonstrated a better zinc utilisation.

1. Introduction

A major problem with porous zinc electrodes for use in secondary power sources is shape change: the redistribution of electrode material with cycling. This occurs because the distribution of zinc replaced in charge never quite matches the distribution of its loss in discharge into the solution. There seems to be no single cause of shape change, and several contributing factors have been proposed [1, 2]. One direct approach to the shape change problem is to incorporate a polymer binder, which stabilises the mobile active material by providing a structural framework. PTFE [1 - 4] is a common additive, though poly(vinyl alcohol) [5] and poly(ethylene) [3] have also been used.

No attention seems to have been paid, however, to the incorporation of polymers by the solution route. We have already reported a study of the

0378-7753/85/$3 30

steady state polarisation behaviour of plain (polymer-free) porous zinc, using a microcomputer-controlled rotating disc electrode (RDE) [6] and have now used this approach to examine a variety of electrode materials incorporating polymers via the solution route. The steady state polarisation experiments were complemented by a study of the short-term relaxation behaviour of some of these materials. This work has been done in conjunction with a programme of cycling experiments on these materials [7].

2. Experimental procedure and equipment

2 1 Materials and electrode preparation

The preparation of polymer-free porous zinc electrodes has already been described in full [6]. Porous zinc electrodes were also prepared incorporating a range of characterised polymers, including (1) poly(styrene) (PS) — supplied by RAPRA*, code PS1, $\bar{M}_N = 103\,000$; (2) poly(methyl methacrylate) (PMA) — RAPRA code PMMA1, $\bar{M}_N = 52\,000$; (3) poly(vinyl chloride) (PVC) — RAPRA code PVC1, $\bar{M}_N = 39\,000$; (4) poly(carbonate) (PC) — RAPRA code PC1, $\bar{M}_N = 15\,000$, (5) poly(vinyl acetate) (PVA) — supplied by BDH, molecular weight ~45 000, (6) poly(isoprene) (PI) — type 1206 supplied by Petrochim., (7) poly(ethylene) (PE) — 'Alkathene', supplied by ICI, and (8) acrylonitrile-styrene (AS) — 'Lustran', supplied by Monsanto.

PS, PMA, PVC, PVA and AS were all incorporated in the pastes as solutions in tetrahydrofuran (THF, Analar, 0.1% quinol stabilised). PC and PI were dissolved in chloroform and in toluene, respectively, and PE was admixed dry. Sufficient polymer solution was added to a dry mix of 25% zinc with 75% zinc oxide to give the required polymer fraction (5%, 10%, 20% or 50% of the dry mix weight) after evaporation of the solvent. Further solvent was added to maintain an excess, together with methanol, which transformed the coarse granular paste to a smooth cream. The addition of methanol was also found to be important in the fabrication of large-area pasted electrodes [7].

This effect of the methanol was investigated by measuring the settled volume of a fixed quantity of zinc powder in a series of dry THF/methanol mixtures. Figure 1 shows how the settled volume of 30 g of zinc powder fell sharply as small additions of methanol were made, stabilising at about 20% by volume. It seems likely that the methanol reduced the surface charge of the zinc particles, enabling them to pack together more closely. Figure 1 makes it clear that the proportion of methanol was not critical, provided it was greater than about 10%, which was always the case. The pastes were introduced into the specially constructed electrode holder [6] (0.4 mm depth × 3 mm diameter), and reduced in 0.01 M KOH solution. The

*Rubber and Plastics Research Association, Shawbury, Shrewsbury, Shropshire, SY4 4NR

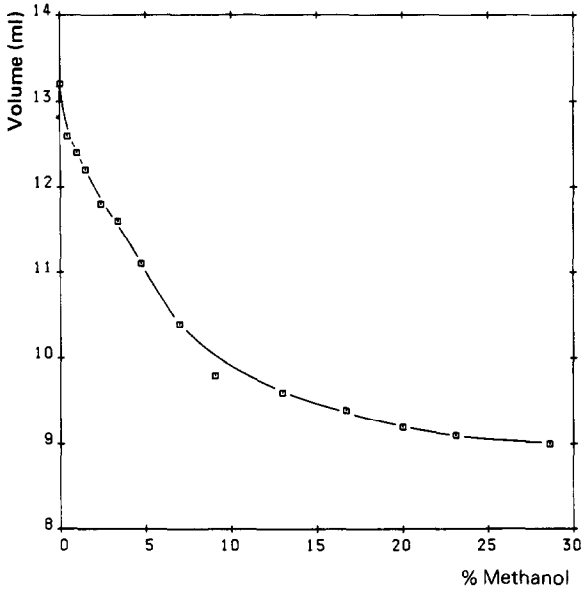

Fig 1 The variation of settled volume of zinc powder (30 g) with methanol concentration in a series of THF/methanol mixtures

polymeric pastes generally showed the same sort of current–time profile as plain zinc [6], though the amount of charge passed in ZnO reduction could not be related to the polymer content; this is discussed later.

2 2 Instrumentation and control

The experimental cell and digital instrumentation are fully described elsewhere [6]. Steady state polarisation behaviour was determined using a microcomputer algorithm, already used successfully on plain porous zinc [6, 8]. The potential E was varied and at each value a sequence of rotation speeds (ω = 3.29, 4.9, 8.12, 15.9 and 44 rev/s) was applied. The steady state anodic dissolution current was determined for each (E, ω) combination.

The same instrumentation was also used to record the transient responses of zinc electrodes. The microcomputer was used to apply the initial potentiostatic perturbation via a digital-to-analogue convertor (DAC, rise time ~1 μs), and to follow the current response either at a slow rate (7 ms sampling time using BASIC programming language), or at a fast rate (60 μs sampling time using machine code programming). At the slow rate current measurements were made at 7 ms intervals for the first 10 s, and thereafter at 1 s intervals. The procedures are described in full elsewhere [8]. Tests with a resistor analogue showed the equipment to be capable of making true current readings within 60 μs of the potential perturbation.

3. Results and discussion

3 1 Steady state polarisation of porous zinc electrodes

3 1 1 Plain porous and poly(styrene)-bonded zinc

It was found that the incorporation of increasing amounts of poly(styrene) (PS) binder progressively suppressed the rotation speed dependence of the anodic dissolution reaction Figure 2 shows i^{-1} *vs* $\omega^{-1/2}$ plots for a Zn/PS20 (i.e. 20% PS) electrode. The plots are linear up to 16 rev/s, beyond which the current increases anomalously. The slope of each plot ($S = d(i^{-1})/d(\omega^{-1/2})$ between 3.29 and 15 9 rev/s decreases with increasing overpotential, to very low values. Figure 3 shows part of the experimental current–time plot for a Zn/PS50 electrode. The very slow equilibration of this electrode at its new potential, and its low sensitivity to rotation speed means that the corresponding i^{-1} *vs* $\omega^{-1/2}$ plots are curved (Fig. 4). Longer equilibration times at $\omega = 0$ mitigated this problem somewhat but at the risk of exhausting the electrode. At higher anodic overpotentials the current was almost independent of the time and of the rotation frequency.

The dependence of the slope S on potential E relates to the mechanism of zinc dissolution, and plain porous zinc has already been found [6] to conform to the findings of Armstrong *et al* [9, 10] for solid zinc. The results for the polymer-bonded electrodes have thrown further light upon the behaviour of these polymer-free electrodes. The porous electrodes prepared in both studies became filled with hydrogen produced by the corrosion reaction and settled at rest potentials in the range $-1400 > E_{rest} > -1425$ (Hg/HgO). Electrode behaviour was consistent in terms of absolute potential rather than overpotential, and the results are presented accordingly.

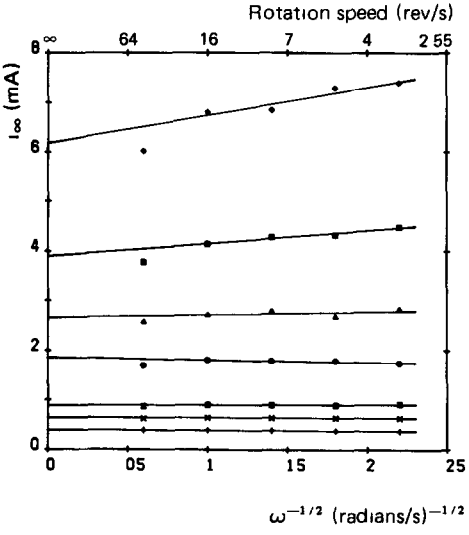

Fig 2 Dependence of current i on rotation speed ω for Zn/PS20 at various anodic potentials, extrapolated to give the notional current i_∞ at infinite rotation speed

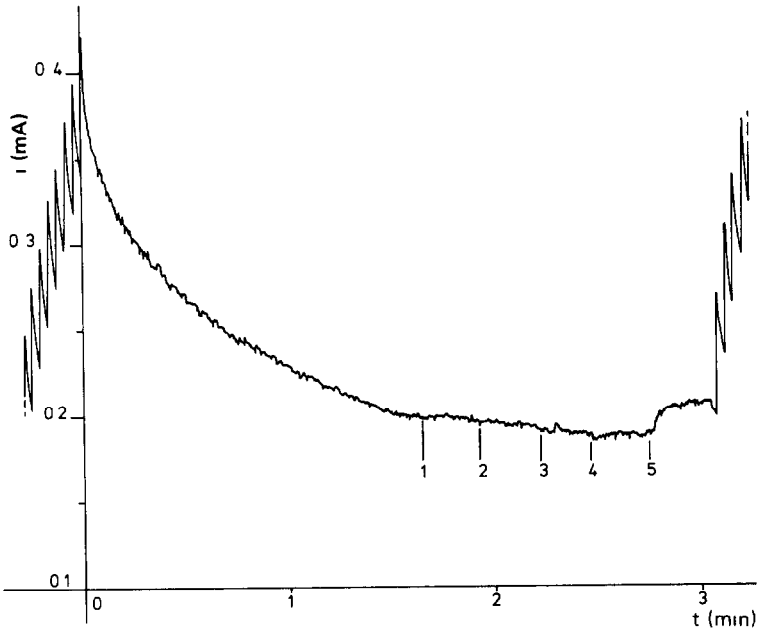

Fig 3 Current *versus* time for Zn/PS50, at $t < 0$ the new potential is set in 10 X 1 mV steps, the electrode equilibrates at zero rev/s and the steady state currents are measured at 3 29 rev/s through to 44 rev/s in succession

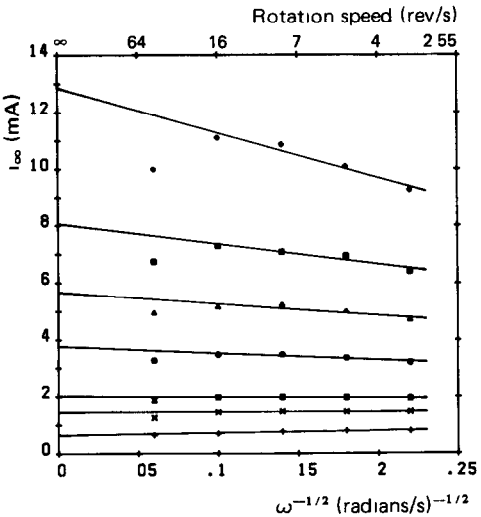

Fig 4 Dependence of current i on rotation ω for the Zn/PS50 electrode used for Fig 3

The theory of the rotating disc electrode (RDE) [11] assumes a planar solid electrode surface with the real area equal to the projected area, so that the electrode reaction proceeds through a planar diffusion layer. The behaviour of the solid zinc RDE [6] conforms to this picture and i^{-1} *vs*

$\omega^{-1/2}$ plots were linear up to rotation speeds of 44 rev/s, beyond which gross turbulence was induced in the cell. The plots for porous electrodes, however, deviated from linearity at high rotation speeds. The slopes of the linear low speed (<16 rev/s) portions of the ι^{-1} *vs* $\omega^{-1/2}$ plots for low overpotentials showed a −30 mV/decade dependence on potential, the same as for solid zinc. The same dependence also holds, however, for the currents passed at the two highest rotation speeds, 15 9 and 44 rev/s. In Fig. 5 the data in in Fig. 10 of ref. 6 are replotted: both for rotation speeds 3.29 - 15.9 rev/s and 15.9 - 44 rev/s. Except for the latter plot lying above the former, they are identical. It seems likely, therefore, that at the highest speed (44 rev/s) the thickness of the diffusion layer is comparable to the scale of the surface roughness, and the layer is beginning to conform to the uneven surface. Hence, one can no longer assume a projected electrode area, but must introduce some roughness factor. Thus, at the highest rotation speeds, the anodic dissolution current is more sensitive to speed, but this behaviour still conforms to the normal, low speed, dissolution kinetics.

At high anodic overpotentials the slope of the steady state polarisation curve (in mV/decade) becomes very large, due to ohmic losses in the electrolyte and to oxide films [6]. Consequently the slope S does not decrease with increasing overpotential as it should, but tends to a limiting low value (Fig. 5).

Figure 6 shows the slope dependences of a range of PS-bonded electrodes. The low polymer electrodes (<10%) behaved like polymer-free electrodes; the ι^{-1} *vs* $\omega^{-1/2}$ plots were linear at low rotation speeds (<16 rev/s), and the corresponding values of S showed a 30 mV/decade potential dependence. With increasing polymer content a large disparity between the low speed and high speed (>16 rev/s) behaviour appears; the high and low

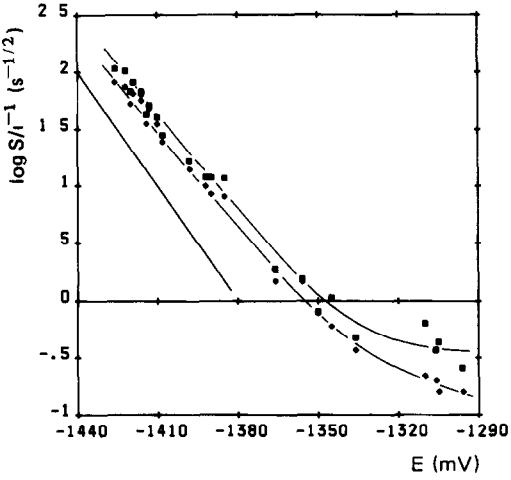

Fig 5 Plots, for plain porous zinc, of log S (where $S = d(\iota^{-1})/d(\omega^{-1/2})$) *vs* potential, with S determined from currents at 3 29, 4 9, 8 1 and 15 9 rev/s (♦), or from 15 9 and 44 rev/s (■) The reference line has a slope of −30 mV/decade

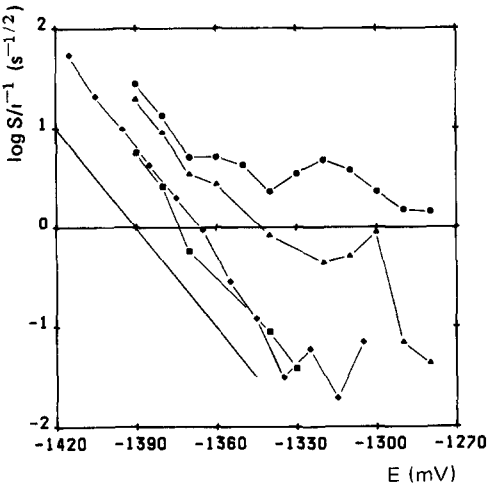

Fig 6 Slope dependences (log S *vs* E) for a range of Zn/PS electrodes comprising ♦, PS5 (low speeds), ■, PS20 (low speeds), ▲, PS20 (high speeds), ●, PS50 (high speeds) The reference line has a slope of −30 mV/decade

speed plots for PS20 are quite separate. The very low speed dependence of the PS50 electrode means that S is negative for low speeds at all potentials, and while S could be positive at high speeds it showed no definite relationship with potential.

The effect of adding PS was to reduce the rotation speed dependence of the anodic reaction but, as we shall see, at the expense of current generation. Within the interior the zinc would become passivated, in the manner observed by Katan *et al* [12] for a pore analogue electrode, by clogging with reaction products. At high rotation speeds, however, local turbulence could introduce fresh electrolyte into the surface pores and re-activate the zinc, as was also seen by Katan *et al* This would suddenly increase the anodic current, in the manner shown for the PS electrodes (Figs 2 and 4). Thus the RDE technique can be used with porous electrodes, but the results must be treated with care, bearing in mind the local perturbations of the hydrodynamic flow pattern caused by the rough electrode surface.

The behaviour of the electrodes themselves could also be complex, depending on how they were treated. Figure 6 shows the behaviour of freshly reduced electrodes. PS electrodes, however, could show quite different polarisation behaviour when tested a second time after resting in the electrolyte solution at open-circuit potential. Figure 7 shows the polarisation behaviour of a PS5 electrode when freshly reduced and when retested after resting disconnected in the solution overnight. In the retest the electrode showed almost no speed dependence, and was much more readily polarised. This behaviour was only seen when the electrodes underwent anodic dissolution before resting in the electrolyte It seems likely that the zincate formed in the electrode in the first experiment was retained and slowly decomposed to ZnO in the manner proposed by Elsdale *et al*

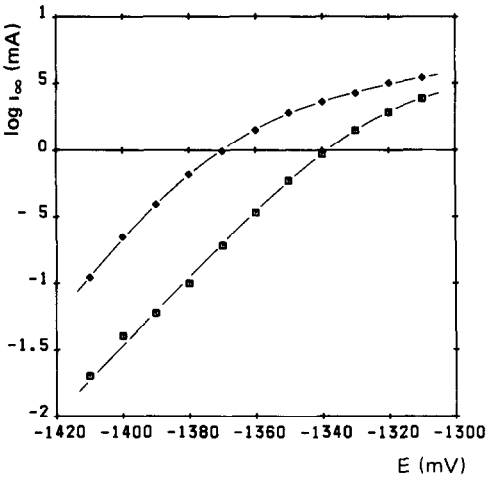

Fig 7 The polarisation behaviour of a Zn/PS5 electrode (♦) in the freshly reduced state, and later (□) after resting at open-circuit in the solution overnight

[13]. The same reaction has been invoked [7] to explain the cycling behaviour of large-format porous polymeric electrodes. The plain zinc electrodes did not show this behaviour, presumably because the zincate, with easier access to the solution, was able to diffuse away.

Figure 8 shows the steady state polarisation curves for the Zn/PS electrodes, derived from measurements of limiting current at low rotation speeds (<16 rev/s), and then extrapolating out diffusion effects. All the plots have the same curved form, with instantaneous Tafel slopes at intermediate potentials of about 80 mV/decade, in agreement with the behaviour

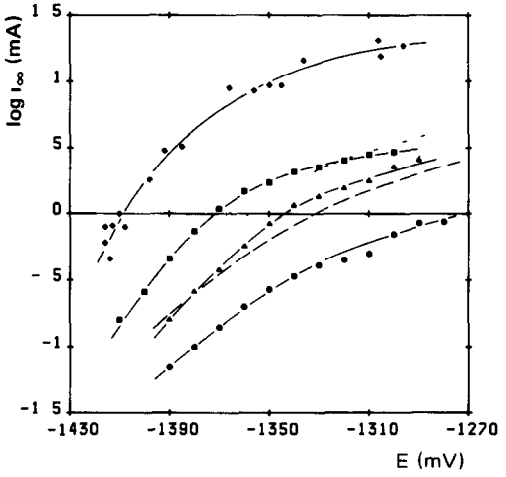

Fig 8 Steady state polarisation curves for Zn/PS electrodes ♦, plain porous zinc, ■, Zn/PS10, ▲, Zn/PS20, ●, Zn/PS50 The broken lines show the "normalised" current curves , Zn/PS10, - - -, Zn/PS20, — — —, Zn/PS50

of polymer-free zinc [6]. The levelling of the plot at the anodic end of the potential range was due to ohmic losses in both the solution and in oxide films within the electrodes. At this point, towards the end of the experimental run, the electrodes were probably undergoing slow passivation, as was seen by Elsdale *et al* [13].

The drastic reduction in anodic current brought about by the addition of PS can be understood in terms of the electrode structure. The morphology of polymer-free porous zinc (Fig. 9) comprises a complex network of zinc granules interconnected by a thread-like form, derived from the reduced ZnO. The large fraction of intervening void space allows easy access to the solution, and would not readily be clogged by oxide. The PS creates a tight three-dimensional net of polymer within which the zinc is dispersed as coarse aggregates (Fig. 10). The zinc area is reduced and the constricted polymer mesh is prone to blockage by oxide, reducing current output and discharge capacity [14]. Moreover, the polymer tends to form a skin over the electrode's free surface (Fig. 11), which further isolates the electrode interior from the solution.

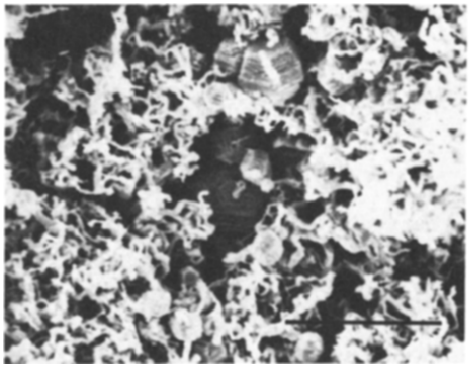

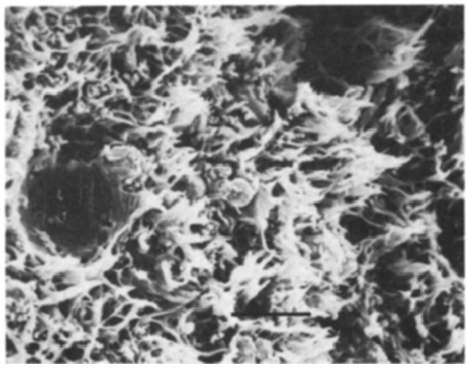

Fig 9 The internal structure of the polymer-free zinc electrode (in this and subsequent micrographs the bar = 10 μm)

Fig 10 The internal structure of the Zn/PS50 electrode

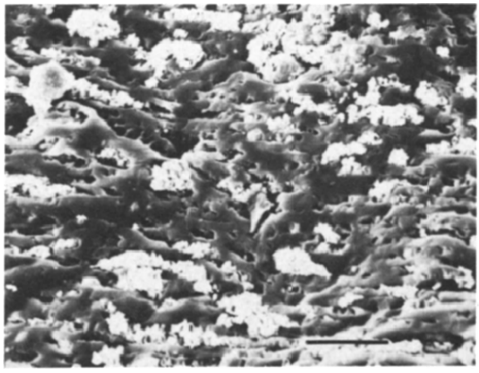

Fig 11 The free surface of the Zn/PS50 electrode

The addition of polymer has another important effect, that of "diluting" the active zinc in the electrode. While this was clearly shown by microscopy, it was not easy to determine the precise zinc content of the polymeric electrodes. Simple coulometric measurements could not be used because the ZnO reduction charge was obscured by the accompanying hydrogen evolution reaction (HER). Measurements of the charge passed in reducing the pastes bore no relation to the polymer content. The zinc contents were therefore calculated from the weights of dried pastes Typical figures for the weights of the Zn/ZnO mix in the PS electrode series were: (1) polymer-free, 4.8 mg (in good agreement with ref. 6); (2) Zn/PS10, 5 7 mg; (3) Zn/PS20, 3.0 mg; and (4) Zn/PS50, 2.0 mg. From simple considerations of density the proportion of zinc in the polymeric pastes should have been much lower. In practice, however, the rapid evaporation of the THF/methanol liquid fraction meant that the fixed cavity volume could accommodate more of the polymeric pastes than of the plain aqueous paste. Thus, the PS10 electrode contained more zinc than the plain electrode, but thereafter the zinc content fell with increasing PS content

Thus, the polarisation curves for the PS electrodes lie closer together, when "normalised" for zinc content, taking the polymer-free electrode as the standard (see Fig. 8). This indicates that the decrease in the zinc content of the polymeric electrodes is counteracted by better zinc utilisation. This effect reveals itself more clearly in the transient experiments, described below.

3 1 2 Comparison of polymer additions

The steady state polarisation behaviour of the full range of polymeric materials tested is shown in Figs. 12 - 15. Current–potential curves (not corrected for zinc content) were determined from the low rotation speed behaviour. The polymeric materials fall into two classes: class 1 (PC, PE and PI), which have little or no effect on current; and class 2 (PS, PMA, PVC and AS), which reduce it significantly. PVA falls somewhere between these two classes. The curves all have the same overall shape as that for plain zinc [6].

This classification also applies to the slope dependence on potential (Figs. 14 and 15). While most additions slightly reduced the slope S at low anodic overpotentials, only the class 2 polymers continued this trend to high overpotentials. All the polymeric materials showed slope dependences at low anodic overpotentials close to the figure of −30 mV/decade found for solid and plain porous zinc [6]. The class 2 polymers maintain this dependence to high anodic overpotentials, producing very low values of S (as low as 0 01), but, inevitably, with a fair amount of scatter. The slope dependence of the class 1 polymers changes at moderate overpotentials, probably because of the higher currents passed, with greater ohmic losses in solution.

The polarisation behaviour of solid zinc, as determined by the steady state RDE technique, matches the recent measurements made by Hendrikx

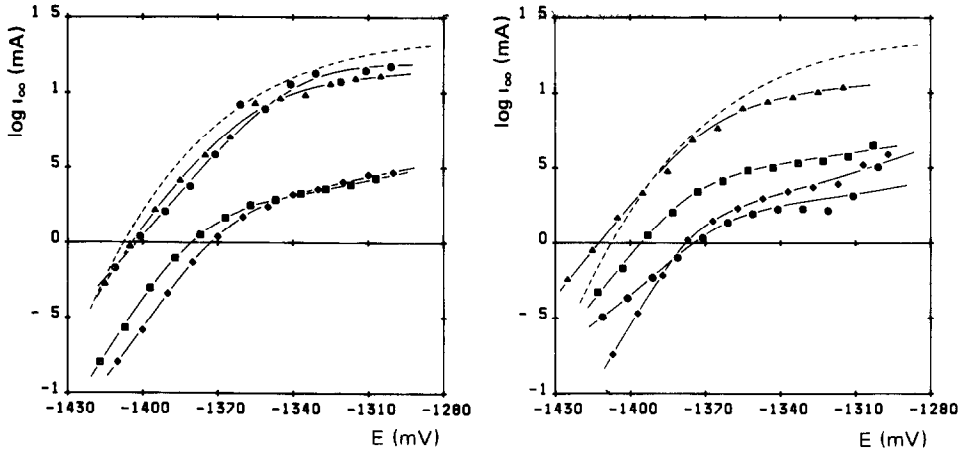

Fig 12 The polarisation behaviour of a range of polymeric electrode materials, incorporating ♦, PS, □, PMA, ▲, PC, and ○, PE, all at the 10% level, — — —, represents the plain zinc electrode (plotted in full in Fig 8)

Fig 13 The polarisation behaviour of a range of polymeric electrode materials, incorporating ♦, PVC, □, PVA, ▲, PI, ○, AS, all at the 10% level, — — —, represents the plain zinc electrode

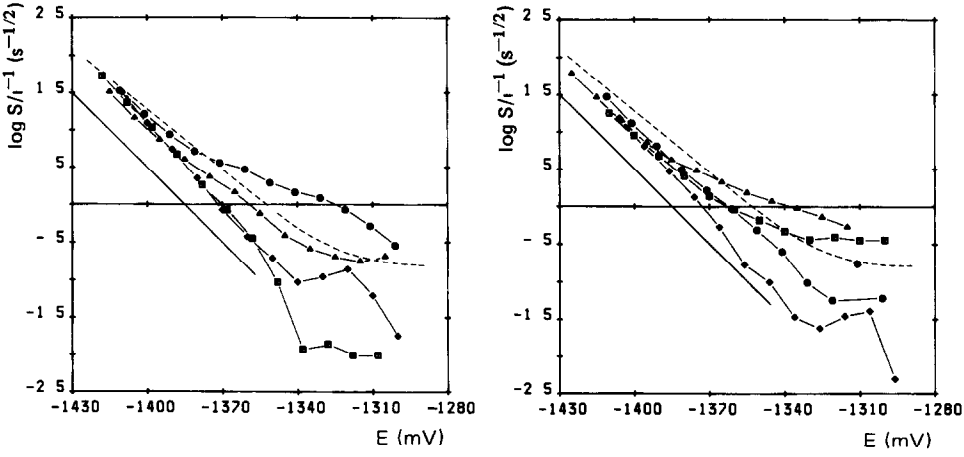

Fig 14 Slope dependence plots for the range of polymeric materials given in Fig 12, the reference line has a slope of −30 mV/decade

Fig 15 Slope dependence plots for the range of polymeric materials given in Fig 13

et al [15] using a transient galvanostatic technique. The steady state polarisation measurements can also be related to the long-term cycling behaviour of these electrode materials, which was investigated in a parallel study [7]. The class 2 polymers, which here reduced the anodic current, in all but one case reduced the electrode cycle life. The class 1 polymers, together with

PVA, were all able to increase the cycle life, though this benefit was lost as their concentration increased. These effects can be related to the structures of the polymeric zinc electrodes, illustrated here (Figs. 9 - 11) for the PS electrodes, and discussed elsewhere [7] for the full range of polymer additions.

3 2 Transient polarisation behaviour

The transient responses of the porous electrodes, rotating at a speed of 10 Hz, to a standard 100 mV anodic step were recorded digitally, as described in § 2.2. The fast machine code data logging routine could just detect the double layer charging transient on the solid zinc electrode (Fig. 16), after which the current was very steady, as would be expected. This event was much slower on the porous electrode, owing to the slow penetration of the potential step into the electrode interior. The double layer charging transient was more or less complete by about 1 ms for porous zinc electrodes containing up to 20% PS The transient was rather shorter for the PS50 electrode, in agreement with differential capacitance measurements [16], which indicated a smaller zinc surface area. The current measurements show the PS additions reduce the current significantly, but this picture changes when the measurements are normalised according to actual zinc content, as was done in § 3.1.1 In the short term the zinc is much better utilised in the high polymer electrodes; the PS20 and PS50 electrodes are now comparable with the plain zinc.

Examination of the transient response at longer times (Fig. 17) reveals that the benefit of porosity is quickly lost, and that the incorporation of

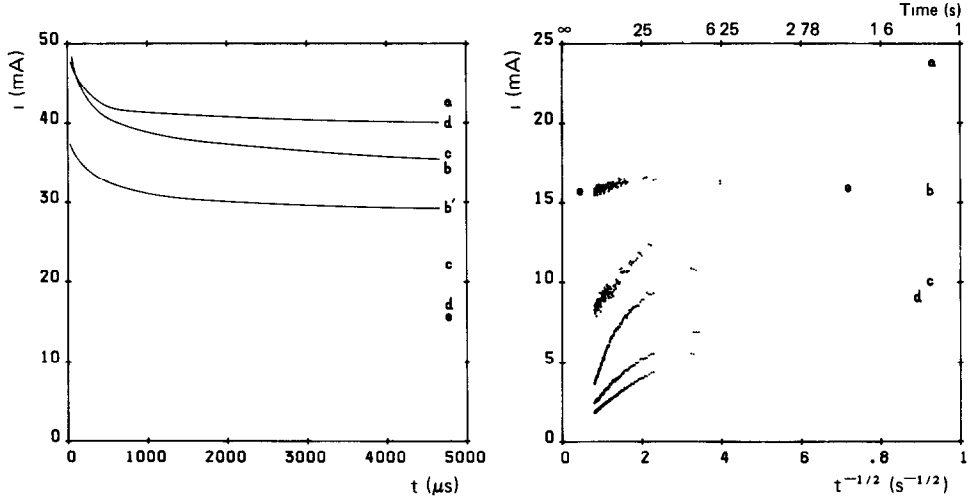

Fig 16 The short-term anodic transient behaviour of the plain and PS-bonded electrodes curve a, plain porous zinc, b, curve (measured), b′ (normalised), Zn/PS10, curve c (measured), c′ (normalised), Zn/PS20, curve d (measured), d′ (normalised), Zn/PS50, curve e, solid zinc

Fig 17 The long-term anodic transient behaviour of the plain and PS-bonded electrodes (legend as for Fig 16)

any amount of PS further retards the anodic reaction rate. Because the anodic currents for the polymeric electrodes approach zero at long times these electrodes do not appear to be losing zinc into solution, but to be being passivated slowly, in the manner observed by Elsdale *et al* [13] for galvanostatic transients on porous electrodes. This is probably due to the anodic reaction at the high overpotential being localised at the front face of the electrode, clogging the structure there and so isolating the interior from the solution [17, 18]. Under these conditions even the plain porous electrode can choke itself, and appear inferior to a solid electrode.

The condition of the actively oxidising electrodes was investigated by applying an anodic potential step, letting the electrode approach a steady state, and then applying the reverse step For solid zinc this produced the brief and finite transient shown in Fig 18. The measured charge passed, 3.6 mC over an area of 0.0707 cm^2, is equivalent to the reduction of about seven monolayers of ZnO [19]. This figure is comparable with the measurements of Armstrong and Bulman [9], made under similar conditions. This is obviously not the compact passivating (type II) oxide film of Powers and Breiter [20], but probably corresponds to the pre-passivation hydroxide film (type I) described by McKubre and Macdonald [21] This thin film seems to cover the electrode continuously, suggested by the linearity of the i *vs* $t^{1/2}$ plot, though continuity is broken by about 0.2 s. Plots of i *vs* $t^{1/2}$ for porous electrodes (Fig. 19) are also linear, but for much longer times, owing to the slow unblocking of the oxide-filled pores. The cathodic current eventually falls to zero when all the zinc is reduced to the metallic state, and the charge passed increases with PS content· 200 mC for plain zinc, 360 mC

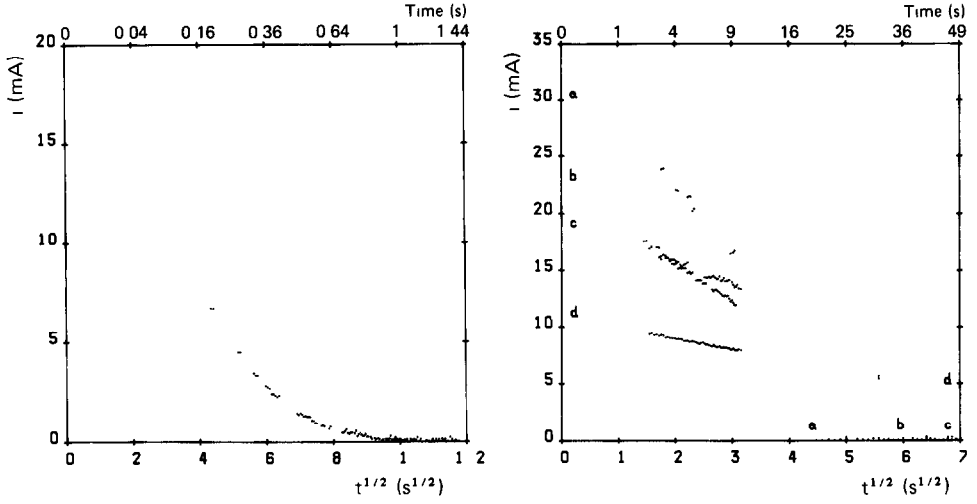

Fig 18 The cathodic transient behaviour of solid zinc The area under the curve is 3 6 mC

Fig 19 The cathodic transient behaviour of plain porous and PS-bonded electrodes curve a, plain porous zinc, total area under curve = 200 mC, b, Zn/PS10, 360 mC, c, Zn/PS20, 400 mC, d, Zn/PS50, 480 mC

for Zn/PS10, 400 mC for Zn/PS20, and 480 mC for Zn/PS50. The retention of oxide has already been seen in the very low rotation speed dependence of the anodic reaction for the PS-bonded electrodes. This behaviour is due to the cellular internal structure and surface skin of the PS electrode.

The performance of the porous electrodes under repetitive cycling conditions was also examined. Both plain and porous zinc showed the same form of response to repetitive anodic potential steps (Fig. 20). In these experiments the electrodes were cycled in a sequence of anodic potential steps, interspersed by equal cathodic potential steps in which the electrode was fully reduced. The plain zinc electrode in each anodic potential step appeared to be approaching a steady long-term current. As the electrode was cycled and the structure became more open and less able to retain ZnO, the i *vs* $t^{-1/2}$ plot started to level out in less time. The PS50 electrode passes much less current and gets blocked in the course of time so that the current always approaches zero at long times.

The response of the plain zinc porous electrodes to repetitive cathodic potential steps is shown in Fig. 21 Here each intervening anodic potential step removed 1 C of charge from the electrode, settling at a steady anodic current before the next cathodic potential step was applied. The amount of oxidised zinc retained within the electrode falls with cycling. The form of the transients remains constant, however, the current only briefly being linear with $t^{1/2}$, and thereafter decreasing faster to be linear with t. It is possible that the early progress of the reaction front into the electrode was assisted by the forced convection due to rotation, and that this rate of progress could not be sustained deeper within the electrode. The behaviour

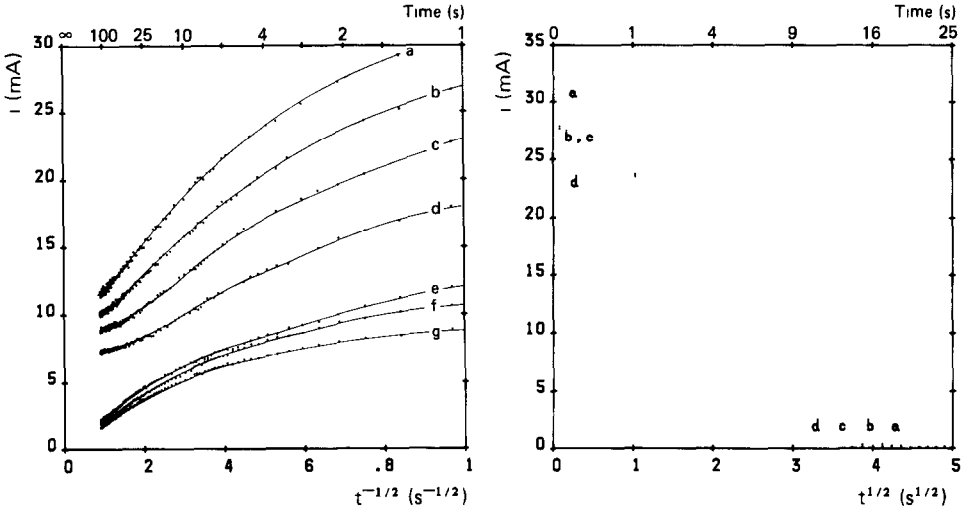

Fig 20 Repetitive anodic current transients on plain porous zinc curve a, 1st, b, 2nd, c, 4th, d, 7th, and on Zn/PS50 curve e, 1st, f, 2nd, g, 4th

Fig 21 Repetitive cathodic current transients on plain porous zinc curve a, 1st, total cathodic charge passed = 290 mC, b, 3rd, 230 mC, c, 4th, 190 mC, d, 6th, 130 mC

of the PS50 electrode with repetitive cathodic potential steps was different (Fig. 22). There was a longer initial period over which the current was proportional to $t^{1/2}$, followed by a period during which the relationship between i and t was complex. It seems likely that we see here the effects of depletion of zinc within the polymer matrix, especially near the electrode surface. With each successive cathodic reduction the initial current is lower and the full reduction takes longer to complete, though there is no marked change in the total charge passed. Furthermore, the forms of the curves are interesting. The fresh PS50 electrode (Fig. 22, curve a) behaves like the plain zinc electrode (Fig. 21), and like the fresh PS-bonded electrodes in Fig. 19. After cycling (Fig. 22, curve d), with loss of surface zinc the current initially decreases rapidly, but then the slope $di/d(t^{1/2})$ decreases, and the current falls more slowly as a greater concentration of zinc is encountered within the electrode.

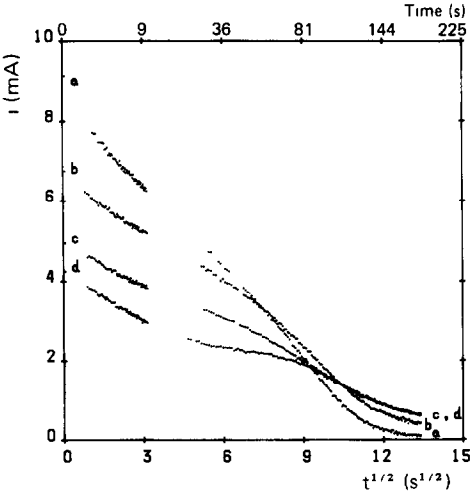

Fig 22 Repetitive cathodic transients on the PS50 electrode curve a, 1st, total cathodic charge passed = 430 mC, b, 2nd, 470 mC, c, 3rd, 450 mC, d, 4th, 400 mC

4. Résumé and Conclusions

The RDE technique can be used to determine the steady state polarisation behaviour of porous electrodes, though the results must be interpreted with care. Polarisation measurements on a number of polymers, incorporated by a soluble route, suggest that the binders form two classes: (1) those which leave the current and slope dependence more or less unchanged, and (2) those which significantly reduce current and also maintain, or even increase, the slope dependence. These latter polymers appear to suppress the rotation speed dependence of the anodic reaction by isolating the zinc within the electrode from the solution. This classification, based on short-term polarisa-

tion measurements can also be related to the performance of polymer binders in a cycling regime. The suppression of speed dependence is associated with severe reduction in cycle life.

While increasing additions of PS markedly reduce the steady state anodic current delivered by the electrode as a whole, there is better utilisation of the smaller zinc content, albeit in the short term. In the longer term the porous electrodes perform badly because the reaction is confined to a thin sub-surface layer which becomes clogged, so that the current tends to zero at long times. Cathodic transients reveal how much the incorporation of PS improves the retention of oxidised zinc. The behaviour of plain zinc under a repetitive perturbation regime changed only little, with steady loss of material and degradation of the porous structure. The polymeric electrodes changed markedly, and this was ascribed to the depletion of zinc within the polymer matrix, especially near the surface.

Acknowledgements

We would like to thank Mr. A. Duffield for helpful discussions of the experimental results. We are grateful to SERC for financial support (A.J S.M.)

References

1 N A Hampson and A J S McNeil, *Electrochemistry*, Specialist Periodical Reviews, Vol 8, 1983, Royal Soc Chem , London
2 J McBreen and E J Cairns, *Adv Electrochem Electrochem Eng , 11* (1978) 273
3 M Cenek, O Kouřil, J Šandera, A Toušková and M Calabek, *Power Sources, 6* (1977) 215
4 A Charkey, *Power Sources, 4* (1972) 93
5 S -P Poa and S J Lee, *J Applied Electrochem , 9* (1979) 307
6 A J S McNeil and N A Hampson, *Surf Technol , 19* (1983) 335
7 N A Hampson and A J S McNeil, *J Power Sources, 15* (1985) 261
8 A J S McNeil and P J Mitchell, *Surf Technol* , in press
9 R D Armstrong and G M Bulman, *J Electroanal Chem Interfacial Electrochem , 25* (1970) 121
10 R D Armstrong and M F Bell, *Electrochemistry*, Specialist Periodical Reports, Vol 4, 1974, Roy Soc Chem , London
11 V G Levich, *Physicochemical Hydrodynamics*, Prentice-Hall, Englewood Cliffs, NJ, 1962
12 T Katan, J R Savory and J Perkins, *J Electrochem Soc , 126* (1979) 1835
13 R N Elsdale, N A Hampson, P C Jones and A N Strachan, *J Appl Electrochem , 1* (1971) 213
14 T S Chang, Y Y Wang and C C Wan, *J Power Sources, 10* (1983) 167.
15 J Hendrikx, A van der Putten, W Visscher and E Barendrecht, *Electrochim Acta, 29* (1984) 81
16 P F Maher, A J S McNeil and N A Hampson, *Electrochim Acta, 30* (1985) 947
17 M W Breiter, *Electrochim Acta, 15* (1970) 1297
18 G Coates, N A Hampson, A Marshall and D F Porter, *J Appl Electrochem , 4* (1974) 75
19 R D Armstrong, G M Bulman and H R Thirsk, *J Electroanal Chem Interfacial Electrochem , 22* (1969) 55
20 R W Powers and M W Breiter, *J Electrochem Soc , 116* (1969) 719
21 M C H McKubre and D D Macdonald, *J Electrochem Soc , 128* (1981) 524